Biosensors and Bioelectronics 67 (2015) 224–229

Contents lists available at ScienceDirect

Biosensors and Bioelectronics

journal homepage: www.elsevier.com/locate/bios

Detection of parathion and patulin by quartz-crystal microbalance functionalized by the photonics immobilization technique

Riccardo Funari [a], Bartolomeo Della Ventura [a], Raffaele Carrieri [b], Luigi Morra [b], Ernesto Lahoz [b], Felice Gesuele [a], Carlo Altucci [a], Raffaele Velotta [a,*]

[a] CNISM and Dipartimento di Fisica, Università di Napoli "Federico II", Via Cintia, 26, Naples 80126, Italy
[b] Consiglio per la Ricerca e la Sperimentazione in Agricoltura – Unità di Ricerca per le Colture Alternative al Tabacco, Via P. Vitiello, 108, Scafati 84018, Italy

ARTICLE INFO

Article history:
Received 6 June 2014
Received in revised form
28 July 2014
Accepted 8 August 2014
Available online 19 August 2014

Keywords:
Parathion
Patulin
Immunosensor
Quartz crystal microbalance
Photonics immobilization technique

ABSTRACT

Oriented antibodies are tethered on the gold surface of a quartz crystal microbalance through the photonics immobilization technique so that limit of detection as low as 50 nM and 140 nM are achieved for parathion and patulin, respectively. To make these small analytes detectable by the microbalance, they have been weighed down through a "sandwich protocol" with a second antibody. The specificity against the parathion has been tested by checking the immunosensor response to a mixture of compounds similar to parathion, whereas the specificity against the patulin has been tested with a real sample from apple puree. In both cases, the results are more than satisfactory suggesting interesting outlook for the proposed device.

1. Introduction

The effective detection of small molecular weights analytes is of paramount importance in a wide range of scientific topics like investigating the molecular recognition phenomena and sensing of toxic molecules (Cooper and Singleton, 2007; Geschwindner et al., 2012; Jones et al., 2013; Vashist and Vashist, 2011). In particular, in the field of environmental monitoring it would be of great importance the availability of cost-effective and sensitive tools allowing the detection of low soluble and harmful compounds like steroids, herbicides, pesticides, toxins and combustion products like polycyclic aromatic hydrocarbon (PAH). As case studies to test our approach, we focused on parathion (IUPAC name O,O-diethyl O-4-nitrophenil phosphorothioate, MW=297 Da) and patulin (IUPAC name 4-hydroxy-4,6-dihydrofuro[3,2-c]pyran-2-one, MW=154 Da), which share a relatively low molecular weight and high interest for environment and health safety. Parathion is an organophosphate pesticide widely used to enhance agricultural production, but for its toxicity (Milles and Salt, 1950) it is now forbidden within the European Union which sets the limits of pesticide residues in food between 50 and 100 μg/kg (Commission Regulation (EC) no. 839/2008). Patulin is an example of mycotoxin which is most likely to be found in crops as a result of fungal infection. Both molecules are highly resistant to degradation and the patulin high toxicity for human and animal health has been recently pointed out in a review by Puel et al. (2010). Patulin level in food is strictly regulated in European countries (Commission Regulation (EC) no. 1881/2006) which set a maximum level of 50 μg/kg for fruit juices and derived products, 25 μg/kg for solid apple products and 10 μg/kg for baby foods. Both parathion and patulin are usually quantified by exploiting expensive, time consuming and relatively complex techniques like high-performance-liquid-chromatography (HPLC) and/or mass spectrometry [see (Blasco et al., 2004; Carabias Martinez et al., 1992; Kwakman et al., 1992) for parathion and (Berthiller et al., 2014; Pereira et al., 2014) for patulin]. Thus, the lack of any commercial and standard immunochemical methods underpins the research for biosensor based detection allowing *in situ* and real-time analysis for environmental monitoring and food quality control.

Amperometric devices are used for parathion in view of their feature to provide cheap, rapid and effective analysis of aqueous samples if the molecules to be detected are electroactive. Zen et al. (1999) developed a sensitive technique for the detection of parathion using a Nafion-coated glassycarbon electrode thus reaching a limit of detection (LOD) of 50 nM. Other sensing strategies are based on electrodes functionalized using enzymes like organophosphorus hydrolase. Exploiting this principle Mulchandani et al. (2001) were able to detect methyl-parathion and paraoxon with a LOD of 20 nM. Even if this kind of devices

* Corresponding author. Tel.: +39 081 6 76148.
E-mail address: rvelotta@unina.it (R. Velotta).

http://dx.doi.org/10.1016/j.bios.2014.08.020
0956-5663/

offers several advantages for water analysis, electrochemical detection can be easily influenced by other oxidizable molecules eventually present in a real sample.

Electrochemical (Vidal et al., 2013), optical (Pereira et al., 2014) and piezoelectric (Pohanka et al., 2007; Prieto-Simón and Campàs, 2009), sensors and biosensors for the detection of mycotoxins are reported in literature, but quite few results are reported for patulin detection. A fluorescence assay was proposed by De Champdoré et al. (2007) with a LOD of 10 μg/L (less than 0.1 μM), but no test on a real sample was carried out. Damián Chanique et al. (2013) have developed a detection method based on the electrochemical reduction of patulin using glassy carbon electrodes. With this strategy they reached a LOD of 300 nM quantifying patulin in commercial apple juices. Starodub and Slishek (2012) proposed a nano-porosus silicon based immunosensor for measuring the level of patulin and T2 mycotoxin in real samples reaching a sensitivity of about 10 ng/mL for both pollutants. More recently, Pennacchio et al. (2014) proposed a competitive surface plasmon resonance (SPR) based bioassay with an estimated LOD of 0.1 nM, but it is worth noticing that the accuracy of SPR measurements can be influenced by interfering effects like temperature and sample composition fluctuation which produce a change in the refractive index not related to the analyte binding.

In view of their robustness, flexibility and cost-effectiveness, quartz crystal microbalance (QCM) technology has achieved an important role in fields like sensing, material science, environmental monitoring and protein studying (Vashist and Vashist, 2011). It is possible use QCM devices for small molecule detection exploiting several principles and configurations (Cooper and Singleton, 2007). All these advantages led to a wide range of publications involving QCM based detection of both pesticides and mycotoxins. For instance, Bi and Yang (2009) used molecular imprinted monolayers (MIMs) self-assembled onto the QCM gold electrode to effectively detect imidacloprid and thiacloprid pesticides in celery juice. They used an extremely sensitive QCM device getting a LOD of 1 μM. Concerning mycotoxin detection an indirect competitive immunological strategy has been adopted by Jin et al. (2009) for the quantification of aflatoxin B1. They significantly improved the sensitivity of the QCM based biosensor coupling the indirect competitive immunoassay with biocatalyzed deposition amplification using enzyme labeled secondary antibodies. Horseradish peroxidase was used to catalyze the oxidation of 4-chloro-1-naphthol to form an insoluble product which deposits onto the QCM electrode thus resulting in a huge increase in the sensor response. This procedure requires several time consuming incubation steps and allows to reach a LOD of about 32 pM.

Surface functionalization is one the main issue in biosensor development, in fact, recent publications show the strong interest in the research of innovative immobilization and functionalization strategies which provide better sensitivity and lower LOD (Jung et al., 2008; Nicu and Leïchlé, 2008). In particular, protein orientation is of paramount importance for immobilized antibodies which have to well expose their sensitive parts, the so called antigen binding sites, to effectively capture the antigens. Trilling et al. (2013) have recently investigated the relationship between analyte characteristics and capture molecule anchoring showing that the uniform orientation of the recognition elements provides a huge systematic improvement in sensitivity for weak interactions. They observed that the smaller the molecule, the lower the epitope number per analyte and, hence, the more important is the orientation of the sensitive biomolecule. By an appropriate antibody surface functionalization, Funari et al. (2013) were able to use a simple transducer like quartz-crystal microbalance (QCM) to detect a concentration of about 200 nM of parathion. This result was achieved by adopting the photonic immobilization technique (PIT) (Della Ventura et al., 2011), so that a gold surface fully covered by oriented antibodies was realized, but also by "weighing down" the molecule through the complexion of parathion with bovine serum albumin (BSA). Since not all the molecules are able to complex with BSA, in this paper we propose a more general approach leading to higher sensitivity and specificity. Essentially, parathion and patulin are "weighed down" by the same antibodies used for the detection onto QCM, mimicking the so called sandwich configuration widely used in the ELISA assays. To this end, the pollutant sample is mixed with an antibody solution before the latter is conveyed to the QCM and LODs of approximately 50 nM and 140 nM are achieved for parathion and patulin, respectively.

2. Materials and methods

2.1. Chemicals

Parathion (45607) and patulin (P1639) were purchased from Sigma-Aldrich. Anti-parathion (ABIN113883) and anti-patulin (AS11-1699) polyclonal antibodies were purchased as rabbit sera from antibodies-online.com and Agrisera respectively. The type G immunoglobulins were purified using the Protein A Antibody Purification Kit (PURE1A) from Sigma-Aldrich. 5,5′-dithiobis-(2-nitrobenzoic acid) also known as Ellman's reagent (D8130), bovine serum albumin (A2153) and the compounds used for the specificity tests, bisphenol A (239658), p-nonylphenol (46018), dichlorvos (45441), diazinon (45428) and paraoxon (36186), were from Sigma-Aldrich. The pollutant samples were prepared using PBS 1 × buffer solution in the fume hood. Helix water, sulfuric acid 98% and hydrogen peroxide 40% were used for the cleaning procedure of the QCM gold surfaces.

2.2. Patulin extraction from real sample

For the specificity test, we used real samples of patulin extracted from apple puree obtained from apple processing plant. To this end a commercial kit (Polyintell Affinimip® SPE cartridges) was used. The extraction was performed as follows: 10 g of apple puree were treated with 150 μL of a pectinase enzyme solution followed by 10 mL water and mixed. Solution was left at room temperature overnight, or for 2 h at 40 °C, centrifuged at 4500g for 5 min and then filtered with a 0.2 μM filter. This solution is used as the loading solution. SPE Cartridge was conditioned with 2 mL of acetonitrile (ACN), then with 1 mL of deionised water. 5 mL of the loading solution was put in the cartridge, which was subsequently washed with 4 mL of deionized water containing 1% of acetic acid. Water was forced down into the cartridge. The cartridge was treated with 1 mL of $CHCl_3$ and patulin was eluted with 2 mL of ACN containing 1% acetic acid. The SPE procedure lasted approximately 30 min. The elution fraction was then evaporated and dissolved in water containing 0.1% acetic acid. This fraction was submitted to a Perkin Elmer HPLC with UV detector to determine the patulin concentration. The same sample was used in QCM validation analysis.

2.3. UV laser source

The immunoglobulin samples were irradiated using the UV laser pulses provided by a custom femtosecond PHAROS laser system with high tunable pulse repetition rate coupled with a harmonic generator stage (HIRO) which allows the conversion to 515 nm, 343 nm and 258 nm wavelengths of the IR fundamental radiation. Both PHAROS and HIRO were from Light Conversion Ltd.

2.4. Quartz crystals

The quartz oscillators (151218) are from ICM, Oklahoma city (USA). They are AT-CUT quartz with a fundamental frequency of 10 MHz. The crystal and the gold electrode diameters are 1.37 cm and 0.68 cm respectively. The gold surfaces are cleaned by immersing the oscillators for 1 min in a glass beaker containing Piranha solution (5:1 ratio between concentrated sulfuric acid and 40% hydrogen peroxide solution), then the quartzes are washed with helix water. The whole cleaning procedure is performed in the hood and can be repeated 3–4 times before the quartz needs to be changed. The QCM device is a μLibra from Technobiochip, Italy. The gold-quartz wafer is placed on the electronic console and the resonance frequency of the oscillator is monitored by producer released software. The QCM is integrated in a microfluidic circuit consisting of the cell which contains the oscillator, platinum threated silicon tubes and a GILSON peristaltic pump. The volume of the circuit is about 300 μL and the flow rate is 3 μL/s. A gentle cleaning with glycine HCl 0.2 M at pH 2.8 allows the removal of only the antigen without significant loss of the tethered antibodies thus leading to the regeneration of the functionalized gold surface. This procedure can be safely applied approximately three times.

2.5. UV activation of antibody solution

Photonic immobilization technique (PIT) (Della Ventura et al., 2011) is a method to immobilize antibodies onto gold based on the photonic reduction of disulfide bridges in proteins by UV illumination of near aromatic amino acid (Neves-Petersen et al., 2002). PIT leads to antibodies oriented side-up i.e. they expose the Fab onto thiol-reactive surfaces like gold plates. The only requirement for applying this technique is the presence into the protein of a closely spaced tryptophan/cysteine–cysteine (Trp/Cys–Cys) triad which is a typical structural characteristic of the immunoglobulin family (Ioerger et al., 1999). The details of this photonic activation have been recently reported by Neves-Petersen et al. (2012). Basically the UV-excitation of tryptophan can result in its photoionization thus generating solvated electrons which are captured by the near electrophillic species like cystines. In this case the result is the breakage of the disulfide bridge thereby generating new thiol functions (red part in the constant region of the antibody) which can easily react with other free thiol groups or with thiol reactive surfaces like gold plates. The rise of the number of the SH groups onto the protein allows new structural conformation for the immobilized immunoglobulin which are characterized by a well exposure of the antigen binding sites thus greatly improving sensor sensitivity. It is well known that UV radiation strongly affects both structure and activity of biomolecules, but we have recently demonstrated that the photonic activation of immunoglobulins by femtosecond UV pulses does not affect their ability to capture the antigen (Funari et al., 2013; Lettieri et al., 2014).

To realize the PIT, antibody samples of 500 μL with a protein concentration of 50 μg/mL were activated using the UV laser source previously described (Fig. 1). In order to find the irradiation conditions which maximize the number of thiol groups per molecule we exploited the so called Ellman's assay (Ellman, 1959) (data not shown). For both anti-parathion and anti-patulin antibodies, the irradiation conditions are $\lambda = 258$ nm, 10 kHz repetition rate, 250 mW of average power, and 1 min irradiation time.

2.6. QCM measurements

Before the experiment each pollutant sample has been incubated for 30 min with the same volume of immunoglobulin solution at a fixed concentration (25 μg/mL), corresponding to an initial concentration of Ab_{free} (*free* antibody in solution) of $[Ab_{free}]_0 \approx 0.17$ μM. This mixture is then tested by the QCM based immunosensor. The experimental procedure consists in the flowing of different solutions onto the gold sensitive surface of the crystal using the fluidic apparatus previously described. Typical QCM outputs involving either irradiated or non-irradiated antibodies in the detection of parathion are shown in Fig. 2.

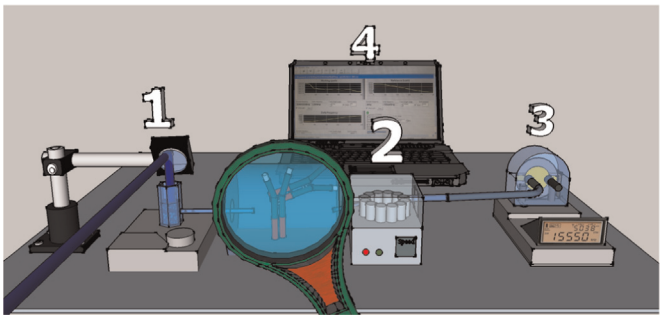

Fig. 1. Experimental layout for PIT. The antibodies are "activated" in the cuvette (1) and conveyed through a peristaltic pump (2) to the QCM (3). The electronics of the QCM is interfaced with a PC (4) so that the frequency shift due to the antibody tethering is controlled in real time. The white end of the antibodies in the pipe is the antigen binding site, whereas the red part highlights the region where the free thiols are produced. (For interpretation of the references to color in this figure legend, the reader is referred to the web version of this article.)

The first step is the reaching of the basal frequency stabilization by flowing PBS solution. Then the surface is functionalized using either irradiated or non-irradiated antibody sample. This step gives rise to a first frequency drop of about 140 Hz, which is the same in both conditions showing that PIT does not affect significantly the total amount of tethered antibodies. This result is in fair agreement with the surface density measurements reported by Peluso et al. (2003) and can be explained by considering that even oriented side up the antibodies can tether with an arbitrary azimuthal, which prevents the possibility to line them up. Subsequently, a washing step with PBS is used to purge the circuit from the excess of immunoglobulins. Then a BSA solution (50 μg/mL) flows into the cell filling the remaining free space on the gold surface. This blocking step is crucial in order to avoid non-specific

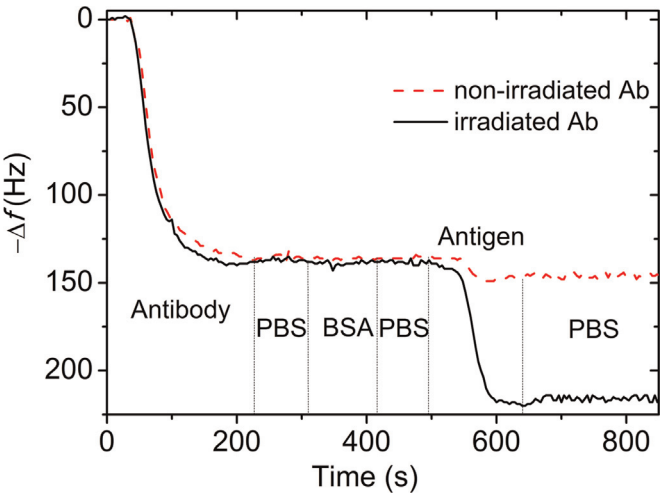

Fig. 2. QCM-based immunosensor outputs for parathion detection using either irradiated (black solid line) or non-irradiated (red dashed line) antibodies. The first frequency shift at about 150 s corresponds to the antibody immobilization onto the sensor surface, while the second drop at about 550 s is due to the detection of analyte–antibody complex (parathion 0.85 μM). The vertical dashed lines highlight the phases of the protocol described in the text. (For interpretation of the references to colour in this figure legend, the reader is referred to the web version of this article.)

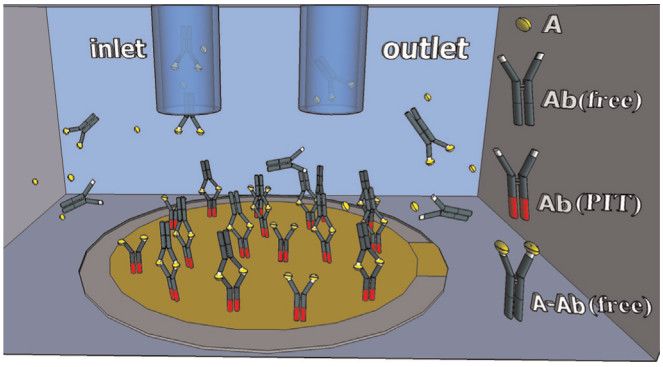

Fig. 3. Sketch of the cell containing the surface detector. The antibodies activated by the PIT are shown with their lower part in red and are tethered side-up on the gold electrode. The solution flowing through the cell contains analyte (small yellow particles) bound to the Ab (green Y-shape), but also "free" Ab and "free" analytes. When a free analyte is recognized by the Ab tethered to the gold, there is no effect on the QCM frequency since the deposited mass is too small. Only when the "sandwich" configuration is realized there is a detectable response. (For interpretation of the references to colour in this figure legend, the reader is referred to the web version of this article.)

interactions between the further flowing molecules and the gold plate. It is worth notice that this phase results in a negligible change in the resonance frequency, therefore proving that the gold surface is quite completely covered by the antibodies. After another cleaning step with PBS, the analyte–antibody sample flows into the circuit and the labeled antigens are captured by the immobilized antibodies, thus resulting in the second frequency shift. This signal is much bigger when the sensor surface is functionalized using UV activated antibodies. A final washing step is then used to remove weakly bonded analytes.

It is important to highlight that in this scheme three species can interact with the sensor (Fig. 3): A (antigen), A–Ab_{free} (antigen–antibody complex) and Ab_{free} (antibody).

The advantage of the simultaneous injection of the three species (A, Ab_{free} and A–Ab_{free}) rather than the sequential injection of A and Ab_{free}, as it occurs in the "standard sandwich ELISA" protocol (Crowther, 1995), relies in the higher *effective* concentration of the analyte in the interaction volume. In fact, due to the stationary equilibrium conditions occurring in the interaction volume of the QCM, when the antibodies are mixed with the solution to be analyzed, the *effective* antigen concentration in the interaction volume coincides with the antigen concentration in the original solution. On the opposite, when the original solution is injected first into QCM and the antibody is injected in a second step after a necessary washing (as in the "standard sandwich ELISA" protocol), the *effective* antigen concentration is lower since there are no free antigens that could replace those detached from the QCM plate by the free antibodies. This, in turn, leads to a reduction of the QCM frequency shift which we measured to be approximately two. Since the aim of this work was the search for the highest sensitivity, the injection of the solution mixed with antibodies was preferred. The drawback of such an approach relies in the need of high antibody concentration in the original solution so that virtually all the antigens are bound and the probability of finding free antigen is negligible. At antigen concentration much higher than the antibody concentration there will be free antigens that would bind the antibodies tethered to the gold plate. In this case the QCM will not provide a detectable signal because of the low antigen mass giving rise to the so-called "hook effect" which can be shifted to high analyte concentration by simply increasing the antibody concentration (Amarasiri Fernando and Wilson, 1992).

3. Results and discussion

The response of the QCM is proportional to the mass tethered to the electrode (Sauerbrey, 1959) so that through the measurement of the frequency shift $\Delta f([A]_0)$, we measure the concentration of the analyte in the solution. While a detailed description of the process in terms of chemical kinetic would require a complex analysis which should also include the diffusion of the several species, we can easily model the observed dynamics by considering the law of mass action and the free diffusion conditions of our experiment. In fact, in this case a Michaelis–Menten type equation is expected to well describe the process when $[A]_0 \ll [Ab_{free}]_0$:

$$\Delta f([A]_0) = \frac{(\Delta f)_{sat}[A]_0}{K_M + [A]_0} \quad (1)$$

In Eq. (1) $(\Delta f)_{sat}$ contains the instrument response and K_M is the so-called Michaelis–Menten constant. The former parameter includes the number of antibodies tethered on the balance as well as their effectiveness in capturing the analyte, i.e. their orientation, whereas the latter provides an estimation of the linear range of the sensor. As explained in Section 2.6, an excess of analyte concentration in the original solution ($[A]_0 \gg [Ab_{free}]_0$) makes high the probability that tethered antibodies bind the analytes (A) rather than the complexed analytes (A–Ab_{free}), but due to the small mass of the analyte such a recognition does not lead to a measurable frequency shift. Thus, when [A] increases and the

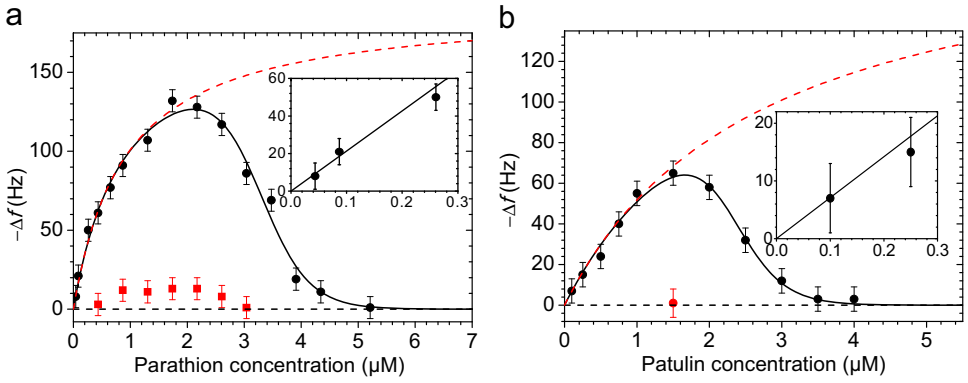

Fig. 4. Response of the QCM to (a) parathion and (b) patulin concentrations when the antibody is irradiated (circle points) and not irradiated (square points). The points achieved with the irradiated antibody are fitted by Eq. (2) (bold line). The low frequency change achieved when the antibody is not irradiated does not allow any significant fit of the experimental data. The inset is the enlargement of the low concentration region, whereas the dashed red lines are the plots of Eq. (1), i.e. the inhibition effect of the free antigens is hampered by high Ab_{free} concentration. (For interpretation of the references to color in this figure legend, the reader is referred to the web version of this article.)

Table 1
Values of the three free parameters as deduced from the best fit of the experimental data.

	K_M [μM]	b [μM]$^{-1}$	$[A]_M$ [μM]
Parathion	0.90 ± 0.05	2.4 ± 0.1	3.3 ± 0.1
Patulin	2.70 ± 0.05	3.0 ± 0.1	2.3 ± 0.1

condition $[A]_0 \approx [Ab_{free}]_0$ is reached an "inhibition effect" starts and further increase of [A] results in a reduction of Δf rather than in its increase. This is observable in Fig. 4 where at low [A] the frequency shift follows Eq. (1), whereas a reduction of the frequency shift occurs at high analyte concentration. A simple way to model the inhibition role played by the free analyte is through a two parameters logistic function, in which one parameter accounts for the analyte concentration at which the inhibition becomes important and the other takes into account the decay rate of the available recognition site. Thus, we can fit our experimental results with the following function:

$$\Delta f([A]_0) = \frac{(\Delta f)_{sat}[A]_0}{K_M + [A]_0} \times \frac{1}{1 + e^{b([A]_0 - [A]_M)}} \quad (2)$$

In the Eq. (2) b and $[A]_M$ are two free parameters accounting for the different kinetics the analytes and antibodies may have, whereas $(\Delta f)_{sat} = 192 \pm 2$ Hz has been determined by measuring the saturation value one measures when a layer of antibodies covers the surface. Although such a value refers to irradiated antibodies, it is essentially the same even when the antibodies are not irradiated (Della Ventura et al., 2011).

The fitting of the experimental results obtained with irradiated antibodies by Eq. (2) (solid black lines in both panels of Fig. 4) provides the results reported in Table 1, while the square red points in Fig. 4 are the results obtained if PIT is not adopted and the antibodies are only tethered spontaneously on the gold. In this latter case it is readily seen that no significant signal is measurable. The dashed red lines in Fig. 4 are the plots of Eq. (1), i.e. the response one obtains when $[Ab_{free}]_0 \gg K_M$, showing that an initial Ab concentration of 1 mg/mL is more than enough in many practical conditions to achieve a monotonic response from our sensor.

The uncertainty in our measurements is due to instrumental limitations in the performances of our QCM as well as to the unavoidable fluctuations in the several steps of the procedure. Assuming an overall error of 10 Hz, (see also the insets in Fig. 4) so that a minimum frequency change $(\Delta f)_{min} = 10$ Hz is required for a measurement to be significantly different from zero, an evaluation of the lower LOD can be obtained by inverting Eq. (1)

$$LOD \approx \frac{(\Delta f)_{min} K_M}{(\Delta f)_{sat}}. \quad (3)$$

Eq. (3) leads to a LOD in water of approximately 50 nM and 140 nM, for parathion and patulin, respectively.

To ascertain the sensor specificity, the same experimental procedure has been used to test the response of the QCM when compounds similar to the analytes to be detected are in the solution. For parathion, we prepared a mixture of bisphenol A (4,4′-(propane-2,2-diyl)diphenol), p-nonylphenol, dichlorvos (2,2-dichlorovinyl dimethyl phosphate), diazinon (O,O-diethyl O-[4-methyl-6-(propan-2-yl)pyrimidin-2-yl] phosphorothioate), and paraoxon (diethyl 4-nitrophenyl phosphate) each of them at a concentration of 2 μM. When only this mixture is made to flow into the QCM no response is provided by the sensor (black solid line in Fig. 5(a)). On the opposite, when parathion at 0.2 μM is added to this mixture, the sensor exhibits a frequency shift of approximately 35 Hz (dashed red line in Fig. 5(a)) in very good agreement with the curve shown in Fig. 4(a) (see the inset), thereby evidencing that pollutants other than parathion have no effect in the QCM response.

As it concerns patulin, Fig. 5(b) reports the QCM response to real samples previously analyzed by HPLC. When there is no patulin in the extract from apple puree, no frequency shift is observed (black solid line); on the opposite, when we analyze extracts from apple puree containing 0.2 μM and 1.0 μM of patulin measured by HPLC, the response of QCM (−12 Hz and −43 Hz, for the two concentrations, respectively) is in very satisfactory agreement with the calibration curve reported in Fig. 4(b). It is worth mentioning, that the real samples we analyzed contained all the possible analytes which could potentially interfere with the patulin measurement; nevertheless, our results show that the technique and the protocol adopted is robust and highly specific.

4. Conclusion

We report here a method to detect light molecules which combines the recently proposed Photonic Immobilization Technique for the antibody functionalization of the gold surfaces, and the antibody-sandwich protocol, to realize an immunosensor based on a QCM. Essentially, in our device the antigen is recognized by its own antibody and the resulting solution is conveyed to the balance. While PIT is shown to largely increase the sensitivity of QCM, the sandwich protocol has a twofold effect: on the one hand it weighs down light molecules, so that they can be "weighed" by QCM, on the other hand it inherently increases even more the

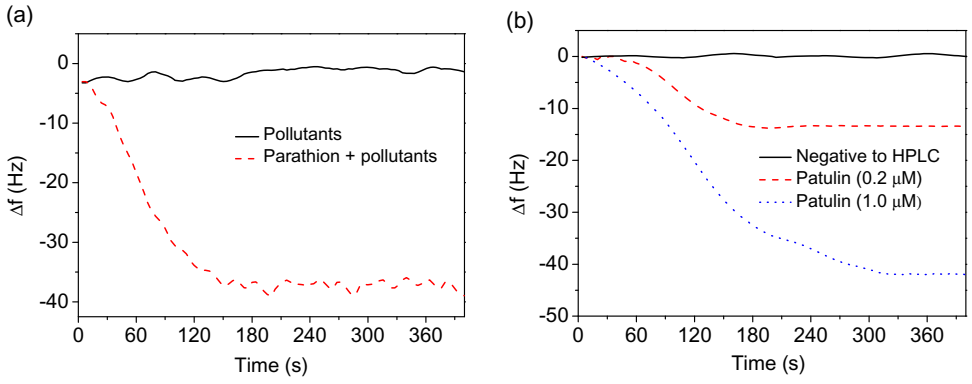

Fig. 5. Sensor specificity i.e.. QCM responses against different pollutants. (a) Parathion at 0.2 μM tested against bisphenol A, p-nonylphenol, dichlorvos, diazinon and paraoxon each of them at 2 μM. (b) Extract from apple puree previously analyzed by HPLC. (—) Negative to patulin; (---) 0.2 μM patulin; (····) 1 μM patulin. (For interpretation of the references to color in this figure, the reader is referred to the web version of this article.)

specificity of the whole device. The sandwich protocol proposed here considers the inclusion of free antibody in the solution to be analyzed, so that the formation of the analyte-antibody complex takes place in the cuvette, and a subsequent injection of the whole solution into QCM. Compared to the typical sandwich ELISA protocol, in which the solution is conveyed as it is to the tethered antibodies and the second antibody is added after a washing, our approach leads to higher sensitivity, the drawback of the decrease of the signal in presence of high analyte concentration being easily overcome by using higher antibody concentration in the mixing volume. On the opposite, one of the advantages of our immunosensors relies in its generality, since in practice antibodies can be produced for any analyte. We have applied our device to parathion and patulin for which LODs of 50 nM and 140 nM were achieved, respectively. In a scenario with lack of simple and reliable immunochemical analysis for two important analytes such as parathion and patulin, our QCM based immunosensor has noticeable advantages in terms of rapidity in the response (only few minutes are required), flexibility and portability, lending itself appropriate for *in situ* analysis.

Acknowledgments

We acknowledge the financial support of the “Fondazione con il Sud” (Project no. 2011-PDR-18, “Biosensori piezoelettrici a risposta in tempo reale per applicazioni ambientali e agro-alimentari”) and the Italian Ministry for Reaserch (MIUR) under the Grant no. PON_0101517.

References

Amarasiri Fernando, S., Wilson, G.S., 1992. J. Immunol. Methods 151, 47–56.
Berthiller, F., Burdaspal, P.A., Crews, C., Iha, M.H., Krska, R., Lattanzio, V.M.T., MacDonald, S., Malone, R.J., Maragos, C., Solfrizzo, M., Stroka, J., Whitaker, T. B., 2014. World Mycotoxin J. 7, 3–33.
Bi, X., Yang, K.-L., 2009. Anal. Chem. 81, 527–532.
Blasco, C., Fernández, M., Picó, Y., Font, G., 2004. J. Chromatogr. A 1030, 77–85.
Carabias Martinez, R., Rodriguez Gonzalo, E., Amigo Moran, M.J., Hernandez Mendez, J., 1992. J. Chromatogr. A 607, 37–45.
Cooper, M.A., Singleton, V.T., 2007. J. Mol. Recognit. 20, 154–184.
Crowther, J.R., 1995. ELISA: Theory and Practice. Humana Press, Totowa, NJ.
Damián Chanique, G., Heraldo Arévalo, A., Alicia Zon, M., Fernández, H., 2013. Talanta 111, 85–92.
De Champdoré, M., Bazzicalupo, P., De Napoli, L., Montesarchio, D., Di Fabio, G., Cocozza, I., Parracino, A., Rossi, M., D'Auria, S., 2007. Anal. Chem. 79, 751–757.
Della Ventura, B., Schiavo, L., Altucci, C., Esposito, R., Velotta, R., 2011. Biomed. Opt. Express 2, 3223–3231.
Ellman, G.L., 1959. Biophysics 82, 70–77.
Funari, R., Della Ventura, B., Schiavo, L., Esposito, R., Altucci, C., Velotta, R., 2013. Anal. Chem. 85, 6392–6397.
Geschwindner, S., Carlsson, J.F., Knecht, W., 2012. Sensors 12, 4311–4323.
Ioerger, T.R., Du, C., Linthicum, D.S., 1999. Mol. Immunol. 36, 373–386.
Jin, X., Jin, X., Liu, X., Chen, L., Jiang, J., Shen, G., Yu, R., 2009. Anal. Chim. Acta 645, 92–97.
Jones, A.M., Grossmann, G., Danielson, J.Å., Sosso, D., Chen, L.-Q., Ho, C.-H., Frommer, W.B., 2013. Curr. Opin. Plant Biol. 16, 389–395.
Jung, Y., Jeong, J.Y., Chung, B.H., 2008. Analyst 133, 697–701.
Kwakman, P.J.M., Vreuls, J.J., Brinkman, U.A.T., Ghijsen, R.T., 1992. Chromatographia 34, 41–47.
Lettieri, S., Avitabile, A., Della Ventura, B., Funari, R., Ambrosio, A., Maddalena, P., Valadan, M., Velotta, R., Altucci, C., 2014. Appl. Phys. A, http://dx.doi.org/10.1007/s00339-014-8340-4, in press.
Milles, H.L., Salt, H.B., 1950. Brit Med. J. 2, 444.
Mulchandani, P., Chen, W., Mulchandani, A., 2001. Sci. Technol. 35, 2562–2565.
Neves-Petersen, M.T., Petersen, S., Gajula, G.P., 2012. In: Satyen Saha (Ed.). UV Light Effects on Proteins: From Photochemistry to Nanomedicine in Molecular Photochemistry: Various Aspects. Tech-Open Access Company. http://dx.doi.org/10.5772/37947. Available from: http://www.intechopen.com/books/molecular-photochemistry-various-aspects/uv-light-effects-on-proteins-from-photochemistry-to-nanomedicine.
Neves-Petersen, M.T., Gryczynski, Z., Lakowicz, J., Fojan, P., Pedersen, S., Petersen, E., Bjørn Petersen, S., 2002. Protein Sci. 11, 588–600.
Nicu, L., Leïchle, T., 2008. J. Appl. Phys. 104, 111101.
Peluso, P., Wilson, D.S., Do, D., Tran, H., Venkatasubbaiah, M., Quincy, D., Heidecker, B., Poindexter, K., Tolani, N., Phelan, M., Witte, K., Jung, L.S., Wagner, P., Nock, S., 2003. Anal. Biochem. 312, 113–124.
Pennacchio, A., Ruggiero, G., Staiano, M., Piccialli, G., Oliviero, G., Lewkowicz, A., Synak, A., Bojarski, P., D'Auria, S., 2014. Opt. Mater. (Amst) 36, 1670–1675.
Pereira, V.L., Fernandes, J.O., Cunha, S.C., 2014. Trends Food Sci. Technol. 36, 96–136.
Pohanka, M., Jun, D., Kuca, K., 2007. Drug Chem. Toxicol. 30, 253–261.
Prieto-Simón, B., Campàs, M., 2009. Monatshefte für Chem. – Chem. Mon. 140, 915–920.
Puel, O., Galtier, P., Oswald, I.P., 2010. Toxins 2, 613–631.
Sauerbrey, G., 1959. Z. Phys. 155, 206–222.
Starodub, N.F., Slishek, N.F., 2012. Adv. Biosens. Bioelectron. 2, 7–15.
Trilling, A.K., Harmsen, M.M., Ruigrok, V.J.B., Zuilhof, H., Beekwilder, J., 2013. Biosens. Bioelectron. 40, 219–226.
Vashist, S.K., Vashist, P., 2011. J. Sensors 2011, 1–13.
Vidal, J.C., Bonel, L., Ezquerra, A., Hernández, S., Bertolín, J.R., Cubel, C., Castillo, J.R., 2013. Biosens. Bioelectron. 49, 146–158.
Zen, J.-M., Jou, J.-J., Senthil Kumar, A., 1999. Anal. Chim. Acta 396, 39–44.